



# Effects of precipitation, irrigation, and exploitation on groundwater geochemical evolution in the people's victory canal irrigation area, China

Zhongpei Liu<sup>1,2</sup> · Shaoyi Feng<sup>1</sup> · Dongqing Zhang<sup>3</sup> · Yuping Han<sup>1,2</sup> · Runxiang Cao<sup>1,2</sup>

Received: 13 June 2022 / Accepted: 28 October 2022 / Published online: 15 November 2022  
© The Author(s) 2022

## Abstract

The People's Victory Canal Irrigation Area is a large gravity irrigation area in the middle and lower reaches of the Yellow River. Groundwater hydrochemistry is controlled by geochemical weathering, precipitation, irrigation from the Yellow River diversion, and artificial exploitation. The Piper diagram, hierarchical cluster analysis, Gibbs diagram, and ion proportion coefficient were applied to improve our understanding of the hydrogeochemical evolution. Our results indicated that groundwater ion concentration has prominent spatial zonation characteristics in the study area. The groundwater ion components in the low salinity area are mainly a result of silicate and carbonate weathering, with the major hydrochemical type being  $\text{HCO}_3\text{-Cl-Na-Mg}$  and  $\text{HCO}_3\text{-Na-Ca}$ . The soil salt content in the low salinity area is low. The main effect of precipitation on groundwater chemical composition is a reduction in groundwater ion concentration by recharge. The groundwater ion concentration near the canal is similar to the Yellow River water. The groundwater ionic components in the high salinity area are mainly affected by weathering, silicate dissolution, and evaporative salt rocks. The water chemical type is  $\text{SO}_4\text{-Cl-Na-Mg}$ . Expectedly, the soil salt content is high in the high salinity area. The Yellow River recharge decreased the ion concentration of groundwater near the canal. In addition, the groundwater exploitation increase results in a change in the flow field, affecting the local groundwater chemistry. The groundwater ion concentration increases as the groundwater flow from the high salinity area to the low salinity area. In contrast, the groundwater ion concentration in the high salinity area decreases. We further discuss these results in the context of the complex influence of precipitation, Yellow River diversion irrigation, and artificial exploitation on the hydrogeochemical evolution.

**Keywords** Groundwater · Hydrochemical characteristics · Influencing factors · The People's Victory Canal Irrigation Area

✉ Zhongpei Liu  
brightlzp@126.com

Shaoyi Feng  
2607592426@qq.com

Dongqing Zhang  
13253631436@163.com

Yuping Han  
han0118@163.com

Runxiang Cao  
runx.cao@foxmail.com

- <sup>1</sup> College of Water Resources, North China University of Water Resources and Electric Power, Zhengzhou 450046, People's Republic of China
- <sup>2</sup> Henan Key Laboratory of Water Resources Conservation and Intensive Utilization in Yellow River Region, Zhengzhou 450046, People's Republic of China
- <sup>3</sup> China Institute of Water Resources and Hydropower Research, Beijing 100038, People's Republic of China

## Introduction

Groundwater is the primary source of water supply in irrigation areas. Understanding the changing laws of the groundwater environment plays a vital role in irrigation, life, and healthy ecological development in irrigation areas (Aksever et al. 2016; Feng et al. 2020). The reduction of water diversion from the Yellow River and excessive groundwater exploitation led to the deterioration of the groundwater environment in irrigated areas (Abdalla et al. 2012; Bodrud-Doza et al. 2016; Liu et al. 2022a, b). In addition, the accumulation of surface soil salinity during the dry seasons and the leaching of soil salinity during the wet seasons further lead to the deterioration of the groundwater environment (Li et al. 2017). The hydrochemical characteristics are the concentrated expression of the groundwater environment (Aragaw et al. 2021; Heleika et al. 2021; Yang et al. 2020),

controlled by multiple factors, including water–rock processes, precipitation, irrigation from the Yellow River, and artificial exploitation. Therefore, groundwater hydrochemical evolution in the irrigation area has the characteristics of complexity, fuzziness, and uncertainty (Khanoranga et al. 2019; Lecomte et al. 2016; Zhang et al. 2019a, b, c).

The evolution of groundwater hydrochemical characteristics largely depends on natural processes, such as hydrogeological conditions, lithology, and water–rock interactions (Cheng et al. 2021; El Alfy et al. 2019; Ran et al. 2018). The hydrochemistry of shallow groundwater in alluvial plains is primarily affected by water–rock interactions with evaporative concentration and ion exchange, also having a significant influence on the groundwater's chemical properties (Ahmad et al. 2020; Ma et al. 2021). Local climate change and human activities also play an irreplaceable role in the evolution of groundwater hydrochemistry (Okkonen et al. 2012; Zhang et al. 2017). Precipitation influences regional groundwater hydrochemistry mainly through two mechanisms. The greater the rainfall amount, the greater the groundwater recharge. As the ion concentration in the precipitation is low with the increased precipitation recharge, the groundwater ion concentration will decrease. On the other hand, the surface soil soluble salt components will enter the aquifer with rain, thus affecting the chemical composition of groundwater (Li 2014; Sharma et al. 2018). The People's Victory Canal Irrigation Area is a Yellow River diversion irrigation area. The groundwater chemical composition in the irrigation area is affected by the magnitude of the Yellow River diversion. Irrigation by the Yellow River will infiltrate and recharge the groundwater, affecting the groundwater quality. Leakage from the Yellow River irrigation also impacts groundwater quality (Asmael et al. 2014; Ben Ammar et al. 2016). In addition, artificial exploitation is the primary groundwater discharge in irrigated areas. The groundwater amount that is exploited is mainly used for agricultural irrigation, followed by livestock watering in rural areas. With variable exploitation, the dynamic field of groundwater will inevitably change, affecting the evolution of groundwater's hydrochemical composition. Thus, the dynamic groundwater environment is resulting in a complex evolution of groundwater hydrochemistry.

The evolution of groundwater hydrochemistry has been extensively studied previously (Wang et al. 2021a, b; Xiong et al. 2020). Many researchers have modeled the aquifer hydrochemistry evolution using multivariate statistical analysis and mineral weathering models in different hydrogeological systems (Keesari et al. 2021; Tyagi et al. 2009; Wang et al. 2018). However, changes in groundwater recharge and discharge conditions could also affect the evolution of groundwater hydrochemistry. So far, few studies have investigated the effects of atmospheric precipitation, water diversion irrigation, and artificial exploitation

on groundwater hydrochemical evolution. Frequently they analyze the influence of only a single factor on groundwater hydrochemistry. Thus, there is a lack of comprehensive studies on the impact of recharge and discharge on hydrochemistry evolution. The association between atmospheric precipitation, water diversion irrigation, artificial exploitation, and groundwater hydrochemical evolution in longer time frames is still unclear.

Therefore, in this study, we focused on the groundwater in the People's Victory Canal Irrigation Area as the research objective. We analyzed the hydrochemical evolution characteristics and the differences between primary ion sources. Our results revealed the influence of atmospheric precipitation, Yellow River diversion irrigation, and artificial exploitation on groundwater chemical evolution in the irrigation area. This paper uses multivariate statistical theory to identify differences or similarities in groundwater hydrochemistry properties. The Gibbs diagram and ion proportionality coefficient method were employed to analyze the natural origin of ion components in groundwater. The influence of precipitation on groundwater hydrochemical components in different areas of study was evaluated by comparing ion concentrations in wet and dry seasons. The correlation between the water amount by the Yellow River diversion, the groundwater depth, and groundwater ion concentration in the longer time frames was investigated. As a result, the mechanisms by which the Yellow River diversion and artificial exploitation influence groundwater chemical evolution in irrigated areas were further assessed.

## Study area

The People's Victory Canal Irrigation Area is a typical agricultural irrigation area in the middle and lower reaches of the Yellow River. It is located between Latitude 35° 00 N–35° 30 N and Longitude 113° 31 E–114° 25 E (Fig. 1), and it covers a 1486.84 km<sup>2</sup> area. The study area consists of the alluvial plain of the Yellow River and the Taihang Mountains piedmont alluvial fan plain. The terrain elevation is higher in the southwest and lowers in the east. The climate in the irrigated area is characterized as a warm temperate continental monsoon. The annual average temperature is 58.1 °F, the annual mean precipitation is 581.2 mm, and the average evaporation is 1864 mm. Precipitation mainly occurs from July to September, which accounts for more than 70% of the total annual rainfall.

Affected by the continuous changes in the Yellow River bank topography, the irrigation area has formed different topographic features such as depressions, floodplains, and river channels. These mainly include the low-lying plain of the original extension, the ancient Yellow River beach, the ancient Yellow River back depressions, the Taihang piedmont

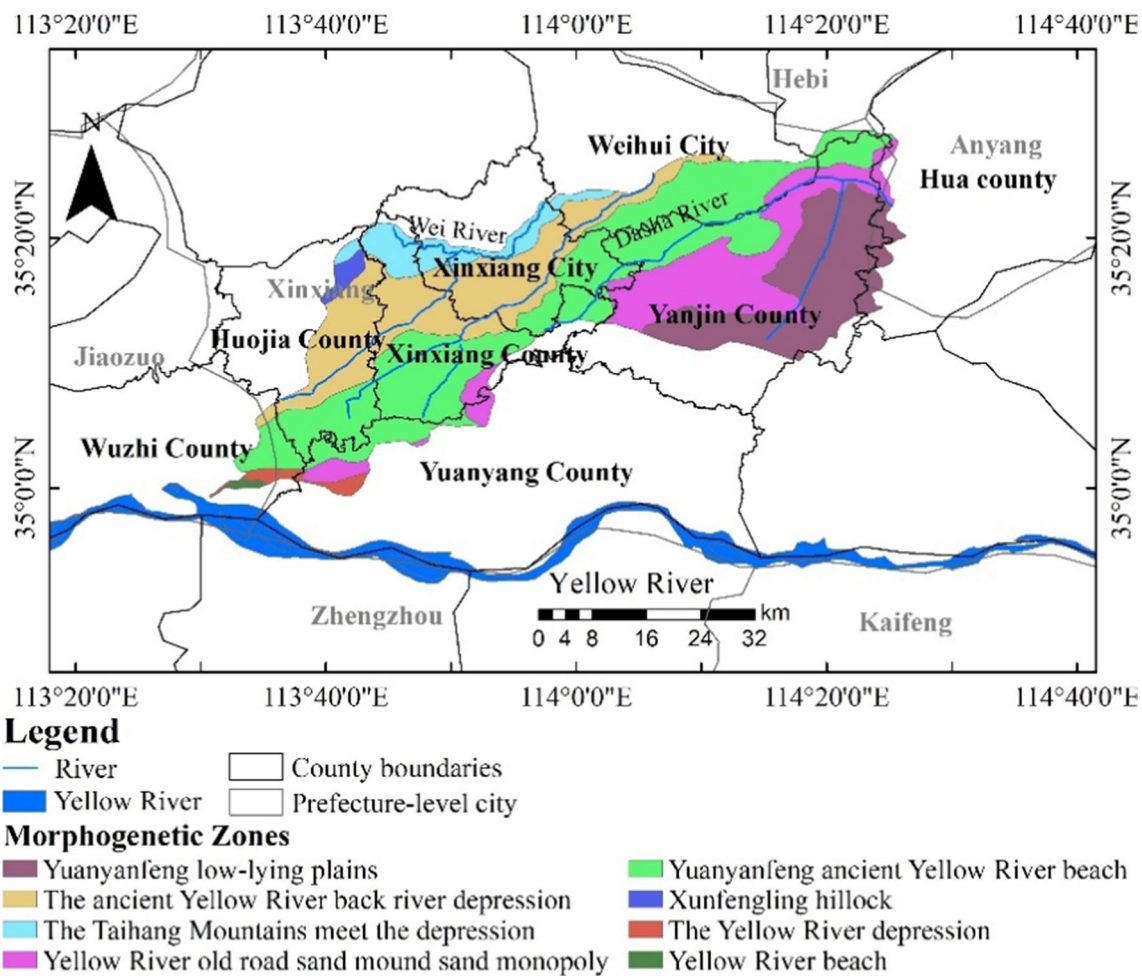


Fig. 1 Study area map

handover depression, the fortress of Sion, and the Yellow River old road sand dune sand monopoly, Yellow River beach and Yellow River back river depression. Initially, during the previous decades, the water used for irrigation was mainly from the Yellow River, and groundwater was used as a supplementary water source. More recently, the water from the Yellow River decreased due to restrictions on the diversion gate height and other factors. The area upstream of the irrigation canal could still use the water from the Yellow River to irrigate farmland. In contrast, groundwater irrigation is primarily used in the downstream area. Since April 1952, the People's Victory Canal Irrigation Area has been operating for 70 years, diverting 39 billion m<sup>3</sup> of water from the Yellow River, with a designed irrigation area of 1228.67 km<sup>2</sup> and an effective irrigation area of 922 km<sup>2</sup>. The crop planting scheme is a winter wheat-summer corn rotation. The irrigation method adopts traditional border irrigation, with a 1200–1800 m<sup>3</sup>/hm<sup>2</sup> irrigation volume. The average depth of the canals in the first year of the irrigation area is about 1–4 m, and the average groundwater depth in the northwest area is about 2–7 m. In 2003, the G33 sampling

point in the middle of the irrigation area formed a depression cone, with the average groundwater depth in this area at about 15 m. The average depth was 4–7 m and 9–14 m before and after 2013, respectively.

## Materials and methods

### Sampling and measurement

The data used in this paper are the groundwater chemistry monitoring data from 1996 to 2013 and 2016 and 2021 in the People's Victory Canal Irrigation Area. The groundwater hydrochemical data from 1989, 1990, 1996 to 2013 were obtained from the monitoring database of the People's Victory Canal Irrigation Administration of Henan Province. The water chemistry data were collected by our research team in 2016 and 2021 using the 425 discrete interval sampler (Solinst, Canada). They were sent to the First Geological and Environmental Survey

Institute of Henan Province for testing within four days. Our research team collected samples for the hydrogen and oxygen isotope data in 2021. The samples were sent to the Isotope Analysis Laboratory, Institute of Geographic Sciences and Natural Resources Research, Chinese Academy of Sciences, for isotope analyses. The soil data used were obtained from the monitoring database of the People's Victory Canal Irrigation Administration of Henan Province from 1993 to 2013. The Yellow River water data were obtained from the sampling data of the People's Victory Canal Irrigation Administration of Henan Province and our research group. The main indicators analyzed in this study were:  $\text{Na}^+ + \text{K}^+$ ,  $\text{Ca}^{2+}$ ,  $\text{Mg}^{2+}$ ,  $\text{SO}_4^{2-}$ ,  $\text{HCO}_3^-$ ,  $\text{Cl}^-$ , electrical conductivity (EC) and total dissolved solids (TDS). The concentration of  $\text{Na}^+$  and  $\text{K}^+$  in water samples was determined by flame atomic absorption spectrometry. The concentrations of  $\text{Ca}^{2+}$  and  $\text{Mg}^{2+}$  were determined by EDTA titration,  $\text{SO}_4^{2-}$  and  $\text{Cl}^-$  ion concentrations were measured by ICS-1100 ion chromatography, and  $\text{HCO}_3^-$  ion concentrations were obtained using acid–base titration with an automatic titrator. All samples passed the charge balance test ( $\leq 5\%$ ), with the accuracy of each index meeting the quality requirements. All TDS and conductivity data points were measured using portable instruments. Hydrogen and oxygen ( $\delta\text{D}$  and  $\delta^{18}\text{O}$ ) stable isotopic compositions were determined by a liquid water isotope analyzer (LGR, USA). The measurement accuracy of  $\delta\text{D}$  and  $\delta^{18}\text{O}$  were  $0.6\text{‰}$  and  $0.2\text{‰}$ , respectively. The sampling point distribution in the study area is summarized in Fig. 2.

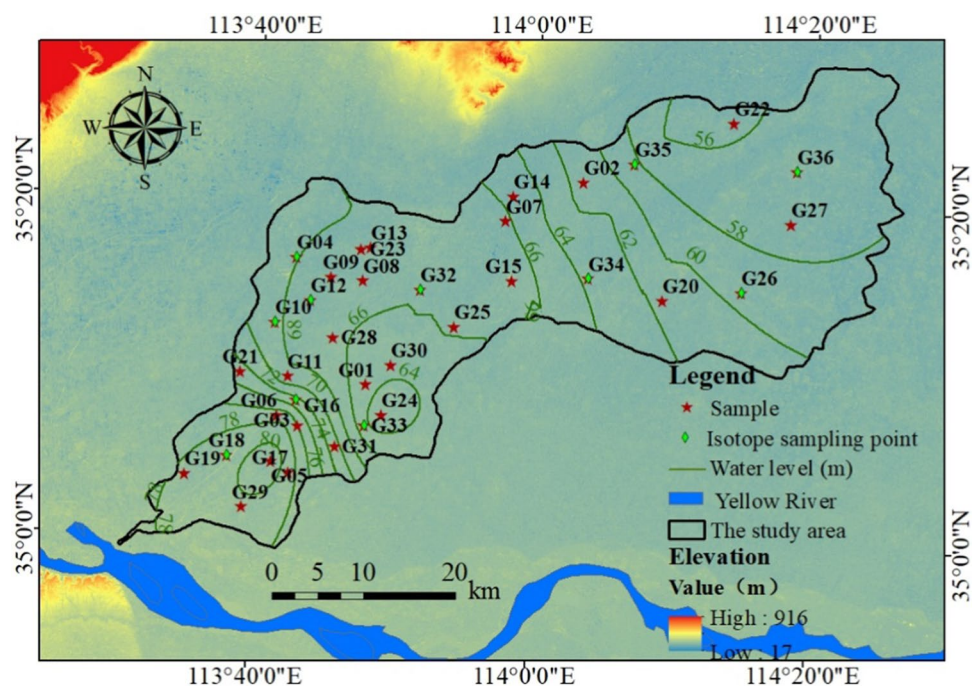
## Analysis of geochemical processes

A Piper diagram was used to study groundwater types and analyze hydrochemical composition processes (Liu et al. 2018a, b; Piper 1944). The Gibbs diagram can identify the composition and variation trends of hydrochemical ions in natural water and determine the degree of hydrochemical formation controlled by precipitation, rock weathering, or evaporation concentration (Qu et al. 2019). To reflect the hydrochemical evolution process and characteristics, one year was chosen for every five years from 1996 as a representative year. Five years in total were selected to analyze the evolution process of groundwater hydrochemistry in the study area.

## Hierarchical cluster analysis

Hierarchical Cluster Analysis classified the groundwater chemical composition using a multivariate statistical analysis approach (Azevedo et al. 2021; Chang et al. 2018; Rahman et al. 2017). All eight hydrogeochemical parameters measured (TDS, EC,  $\text{Na}^+ + \text{K}^+$ ,  $\text{Ca}^{2+}$ ,  $\text{Mg}^{2+}$ ,  $\text{SO}_4^{2-}$ ,  $\text{HCO}_3^-$ ,  $\text{Cl}^-$ ) were implemented in the cluster analysis (Tirumalesh et al. 2010). To prevent the sample distance from being affected by parameter magnitude differences, the Z-score was used to standardize groundwater data. Ward's linkage method and Euclidean distance were used to classify groundwater samples. Then the average values of various groundwater physical and chemical parameters were calculated (Cui et al. 2020; Huang et al. 2021).

**Fig. 2** Location map showing sampling site of the study area



## Isotope mixing model

Stable isotope technology can accurately indicate the material source and the geochemical processes experienced by the geological body. We used a Bayesian mixture model (MixSIAR version 3.1.10) to quantify the contribution ratio of different groundwater recharge sources in the study area (Cui et al. 2021; He et al. 2020; Rodriguez et al. 2016; Tran et al. 2019). The principle is as follows:

$$X_{ij} = \sum_{k=1}^n P_k (S_{jk} + C_{jk}) \varepsilon_{ij}$$

$$S_{jk} \sim N(\mu_{jk}, \omega_{jk}^2)$$

$$C_{jk} \sim N(\lambda_{jk}, \tau_{jk}^2)$$

$$\varepsilon_{ij} \sim N(0, \sigma_j^2)$$

where  $X_{ij}$  is the  $j$ th isotope value in the  $i$ th mixture water sample ( $i, j = 1, 2, 3, \dots, n$ ), and  $k$  is the potential isotope source;  $S_{jk}$  is the  $j$ th isotope value of the  $k$ th endmember,  $\mu_{jk}, \omega_{jk}$  are the mean and standard deviation of  $S_{jk}$ ;  $P_k$  is the contribution ratio of each source, that is calculated by the model;  $C_{jk}$  is the fractionation factor of the  $k$ th endmember on the  $j$  isotope,  $\lambda_{jk}$  is the mean of the fractionation factor,  $\tau_{jk}$  is the standard deviation;  $\varepsilon_{jk}$  is the residual error, which represents the undetermined variable between different single mixtures, the mean is 0, and the standard deviation is  $\sigma_{jk}$ .

Atmospheric precipitation, irrigation from the Yellow River, and artificial exploitation differentially affect the groundwater chemical evolution in the high, and low salinity areas. Representative points were selected in both areas to analyze the differences in the degree of influence. G06 and G11 groundwater sampling points represented low salinity areas, while G09 and G13 groundwater sampling points represented high salinity areas. G06 and G09 are located far from the canal, and G11 and G13 are located far from the canal. However, since the volume of groundwater exploited and used for agricultural irrigation in the study area is not measured, studies so far have shown that the main factor affecting the groundwater depth is artificial exploitation, with the groundwater level declining year by year, showing characteristics of artificial exploitation (Liu et al. 2018a, b). Therefore, this study reveals the influence of exploitation on groundwater hydrochemistry by evaluating the relationship between groundwater depth and hydrochemical composition.

The Hierarchical Cluster Analysis and correlation analysis were carried out using SPSS 22. The Stiff diagram, Piper diagram, Gibbs diagram, and ion ratio diagram were performed in Origin 2021. The study area's geographical positioning and the sampling points distribution map were drawn by ArcGIS 10.3.

## Results and discussion

### Hydrochemical characteristics of groundwater in the irrigation areas

The relationship of cationic concentration in the study area groundwater was as follows:  $\text{Na}^+ + \text{K}^+ > \text{Ca}^{2+} > \text{Mg}^{2+}$  (Fig. 3). The highest  $\text{SO}_4^{2-}$  concentration was observed in the northwest region, while the  $\text{HCO}_3^-$  concentration was higher in the other regions. The lowest ion concentration in groundwater sampling sites was observed in 1996. The  $\text{Na}^+ + \text{K}^+$  mean concentration was 100 mg/L, the mean  $\text{HCO}_3^-$  concentration was 288.87 mg/L, and the mean TDS value was 673.51 mg/L. The highest concentration of ions in groundwater sampling sites was observed in 2021. The average  $\text{Na}^+ + \text{K}^+$  concentration was 206.08 mg/L, the average  $\text{HCO}_3^-$  concentration was 595.96 mg/L, and the average TDS concentration was 1516.36 mg/L, which were about twice the average values of 1996 (Table 1). The spatial concentration distribution of each ion and TDS was not uniform in the study area.  $\text{SO}_4^{2-}$ ,  $\text{Na}^+ + \text{K}^+$ ,  $\text{Cl}^-$ ,  $\text{Mg}^{2+}$  and TDS concentrations were higher in the northwest region than in other regions. The average TDS of groundwater sampling points in the northwest region in 2016 was 3203 mg/L, while in other regions, it was 942 mg/L.

### Spatial clustering characteristics of groundwater in irrigation areas

Q-mode hierarchical cluster analysis divided groundwater samples into two clusters, A and B. Cluster A was further divided into three subsets, A1, A2, and A3 (Fig. 4). The samples in cluster A had a low TDS, with an average of 935.32 mg/L and a range from 194.83 to 2280.10 mg/L. Cluster A groundwater had an extensive distribution area in the study's middle and lower parts and the eastern region. The landform features were mainly the ancient Yellow River beach and Yellow River old road sand dune sand monopoly. Cluster B groundwater had a high TDS, with an average of 3347.16 mg/L and a range from 2596.60 to 4431.50 mg/L. Cluster B groundwater was mainly distributed in the northwest area, and the landform features were the ancient Yellow River back depression and the Taihang piedmont handover depression. After combining cluster analysis results and geomorphological features, the study area was divided into high and low salinity regions (Fig. 5).

The cluster A1 groundwater sampling points were mostly from the low salinity area in 2016 and 2021 and were mainly the  $\text{HCO}_3^-$  water type. The Cluster A3 groundwater sampling points were from the low salinity area from 1996 to 2011 and had a low ion concentration. The relative ratios of hydrochemical ions in Cluster A3 and Cluster A1

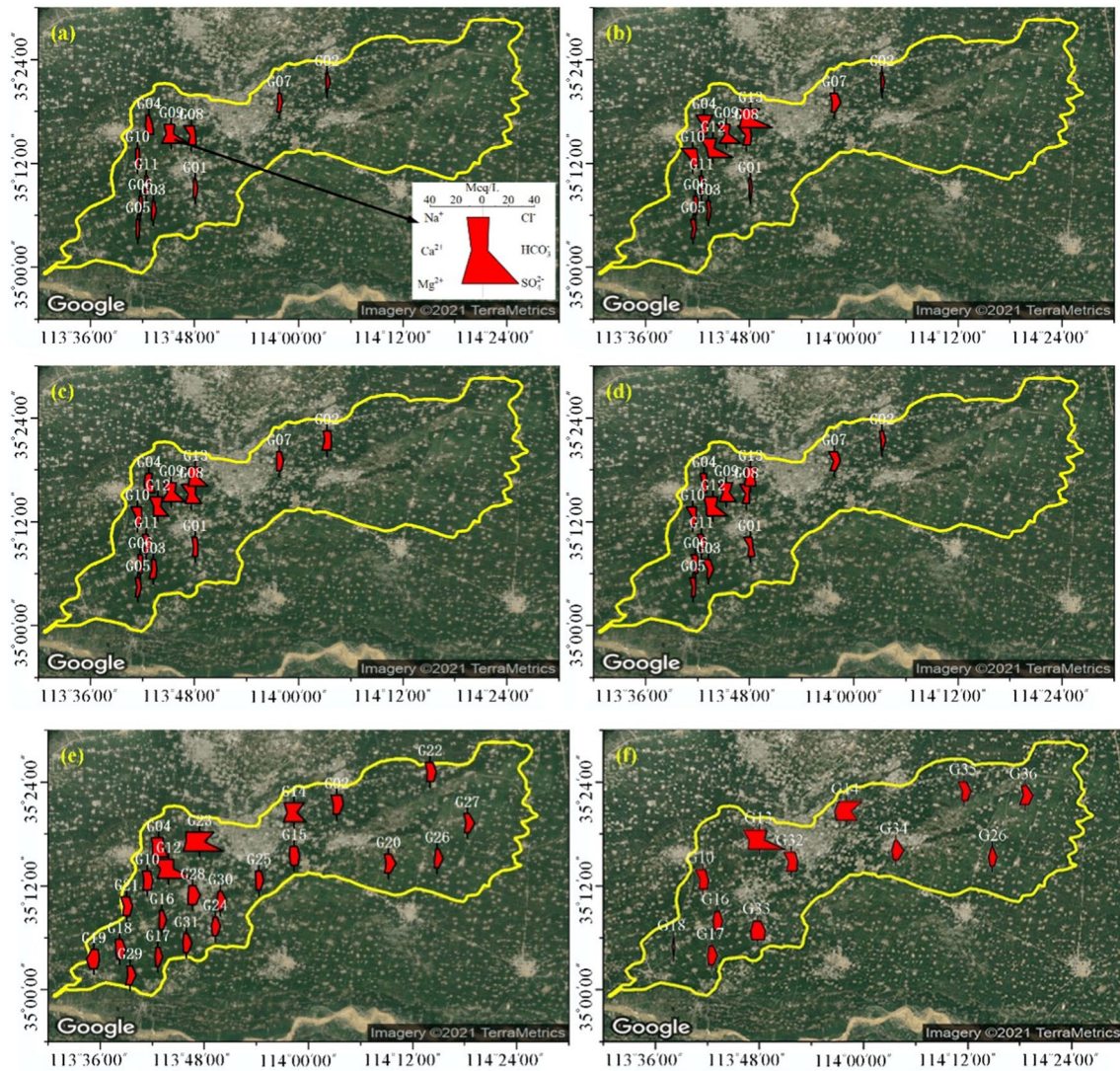


**Fig. 3** The spatial distribution of ion concentrations in groundwater in the study area: **a** 1996, **b** 2001, **c** 2006, **d** 2011, **e** 2016, **f** 2021

groundwater were similar. The ionic abundance followed the order:  $\text{Na}^+ + \text{K}^+ > \text{Mg}^{2+} > \text{Ca}^{2+}$  and  $\text{HCO}_3^- > \text{SO}_4^{2-} > \text{Cl}^-$ . Cluster A2 groundwater comprised the G04, G08, G09 and G10 groundwater sampling points from 1996 to 2011. Compared with the A1 and A3 clusters, the A2 cluster samples  $\text{Na}^+ + \text{K}^+$ ,  $\text{SO}_4^{2-}$ ,  $\text{Cl}^-$  concentration was higher. The G24 groundwater sampling site formed cone of depression at 2001, and the A2 cluster groundwater was affected by groundwater flow from the high salinity area to the low salinity area, increasing the concentration of hydrochemical ions (Liu et al. 2022a, b). Cluster B comprised the G13, and G12 groundwater sampling points from 1996 to 2011 and included the G14, and G23 groundwater sampling points in 2016 and 2021. The ionic abundance followed the order:  $\text{Na}^+ + \text{K}^+ > \text{Mg}^{2+} > \text{Ca}^{2+}$  and  $\text{SO}_4^{2-} > \text{Cl}^- > \text{HCO}_3^-$ . This area

was characterized as a saline-alkali land, and the groundwater salinity was higher than in other areas.

### Groundwater hydrochemical types

The groundwater hydrochemical types in the low salinity area were slightly different from year to year, while in the high salinity area remained stable across the whole period (Fig. 6). The percentage of alkaline-earth metal ions ( $\text{Ca}^{2+} + \text{Mg}^{2+}$ ) was lower compared to the alkaline metal ions ( $\text{Na}^+ + \text{K}^+$ ) in most groundwater samples in 1996, 2001, and 2011. The 1996, 2001, and 2011 groundwater samples from the low salinity area were dominated by the  $\text{HCO}_3\text{-Cl-Na-Mg}$  water type. On the other hand, the hydrochemical type of the high salinity area was  $\text{SO}_4\text{-Na-Mg}$ .

**Table 1** The statistical characteristics of groundwater hydrochemical parameters. All sample concentrations are in mg/L

Years	Statistic values	pH	TDS	Ca <sup>2+</sup>	Mg <sup>2+</sup>	Na <sup>+</sup> + K <sup>+</sup>	Cl <sup>-</sup>	SO <sub>4</sub> <sup>2-</sup>	HCO <sub>3</sub> <sup>-</sup>
1996	Minimum value	8.30	250.15	19.70	23.70	35.50	17.40	16.00	183.50
	Maximum value	8.50	2280.10	175.10	193.20	291.40	175.70	1336.50	445.10
	Mean	8.37	673.51	64.61	53.52	100.40	83.05	231.41	288.87
	Standard deviation	0.06	619.18	43.81	47.99	92.60	51.06	389.24	78.24
	Coefficient of variation	0.01	0.92	0.68	0.90	0.92	0.61	1.68	0.27
2001	Minimum value	7.00	293.30	16.10	1.60	62.70	35.90	44.10	110.10
	Maximum value	8.20	2827.05	219.00	148.00	509.70	512.70	1589.40	649.90
	Mean	7.61	1031.48	55.66	54.75	225.33	163.53	340.25	323.09
	Standard deviation	0.44	777.32	54.40	40.96	160.43	123.72	477.17	161.35
	Coefficient of variation	0.06	0.75	0.98	0.75	0.71	0.76	1.40	0.50
2006	Minimum value	8.20	494.47	30.10	39.30	75.00	79.80	60.90	182.10
	Maximum value	7.20	2223.75	165.70	192.90	379.80	311.20	1069.10	518.80
	Mean	7.48	1059.12	82.35	80.63	181.59	174.33	371.86	356.43
	Standard deviation	0.29	578.04	42.96	42.45	105.00	81.38	331.29	98.75
	Coefficient of variation	0.04	0.55	0.52	0.53	0.58	0.47	0.89	0.28
2011	Minimum value	6.50	392.80	19.40	16.40	103.10	59.80	17.90	248.80
	Maximum value	7.20	2337.56	227.30	137.70	346.40	351.10	1195.60	630.40
	Mean	6.90	961.57	58.34	56.98	218.61	161.89	293.00	363.56
	Standard deviation	0.19	577.50	58.51	40.62	76.94	89.73	348.20	121.64
	Coefficient of variation	0.03	0.60	1.00	0.71	0.35	0.55	1.19	0.33
2016	Minimum value	7.18	652.51	57.25	48.40	74.94	67.11	67.67	327.13
	Maximum value	7.83	4431.50	471.86	331.85	660.51	853.60	2051.30	763.42
	Mean	7.51	1367.90	147.84	98.64	197.34	204.30	404.04	574.02
	Standard deviation	0.15	997.83	92.25	69.96	151.44	189.04	558.45	101.54
	Coefficient of variation	0.02	0.73	0.62	0.71	0.77	0.93	1.38	0.18
2021	Minimum value	7.20	750.70	77.55	52.17	44.77	63.67	168.49	431.17
	Maximum value	8.20	4145.50	406.83	231.83	613.74	903.05	2121.44	841.40
	Mean	7.52	1761.36	188.75	114.46	239.86	277.80	621.78	638.35
	Standard deviation	0.28	1028.24	110.32	61.92	160.14	242.45	567.41	134.40
	Coefficient of variation	0.04	0.58	0.58	0.54	0.67	0.87	0.91	0.21

Ca<sup>2+</sup> + Mg<sup>2+</sup> concentration in groundwater samples in 2006 and 2016 and 2021 was higher than in 2001 and 2011. The percentage of alkaline earth metal ions (Ca<sup>2+</sup> + Mg<sup>2+</sup>) was greater compared to the alkaline metal ions (Na<sup>+</sup> + K<sup>+</sup>). In 2006 and 2016, the groundwater hydrochemical type in the low salinity areas was HCO<sub>3</sub>-Na-Ca, while in the high salinity areas was SO<sub>4</sub>-Cl-Na-Mg. The Yellow River water chemical types were HCO<sub>3</sub>-Cl-Na-Ca and HCO<sub>3</sub>-SO<sub>4</sub>-Ca-Na. In the enlarged view of Fig. 6, the chemical water types of groundwater sampling points near the irrigation canal were similar to the Yellow River water. The canal system's effective utilization coefficient in the irrigation area was only 0.4–0.5, and the Yellow River water leakage was relatively large. The sampling points similar to the Yellow River hydrochemical types were distributed at the head of the canal, indicating that the water leakage and recharge from the Yellow River have a profound impact on groundwater hydrochemistry.

### δD and δ<sup>18</sup>O characteristics of study area water groups and recharge of groundwater

Hydrogen–oxygen stable isotope relationships are essential for groundwater recharge sources and migration processes (Fan et al. 2017; Guo et al. 2022; Liu et al. 2021; Wang et al. 2019; Xu et al. 2022). To analyze the precipitation recharge of groundwater, long-term monthly-scale atmospheric precipitation isotope data from the Zhengzhou Observatory were obtained from the International Atomic Energy Agency. The hydrogen and oxygen stable isotope values in monthly precipitation at Zhengzhou Station varied greatly. The variation ranges of δD and δ<sup>18</sup>O were − 92.8‰ ~ − 4‰ and − 13.15‰ ~ − 0.21‰, respectively, and the weighted averages were − 55.11‰ and − 7.31‰, respectively. Hydrogen and oxygen isotope data in precipitation were used to calculate the local atmospheric precipitation line equation (LMWL): δD = 6.748δ<sup>18</sup>O − 2.71. Its slope was smaller than the global atmospheric precipitation

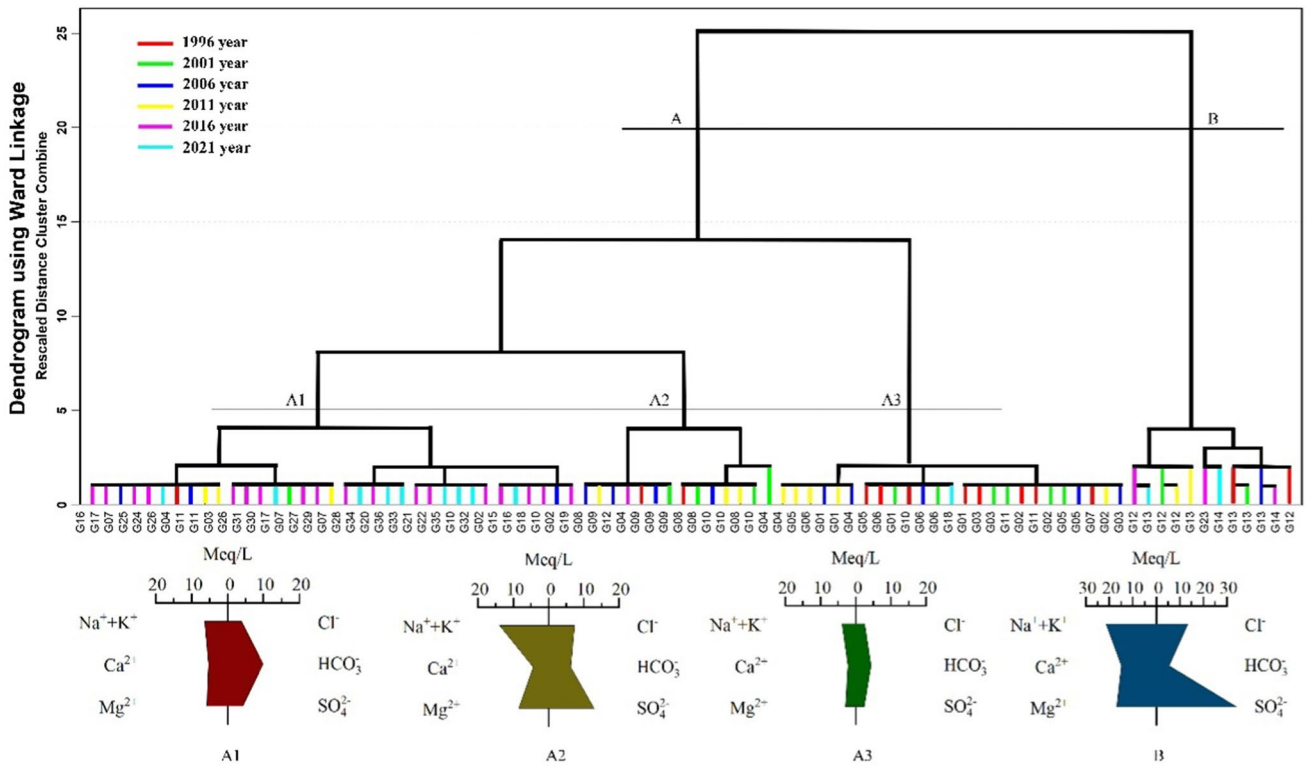
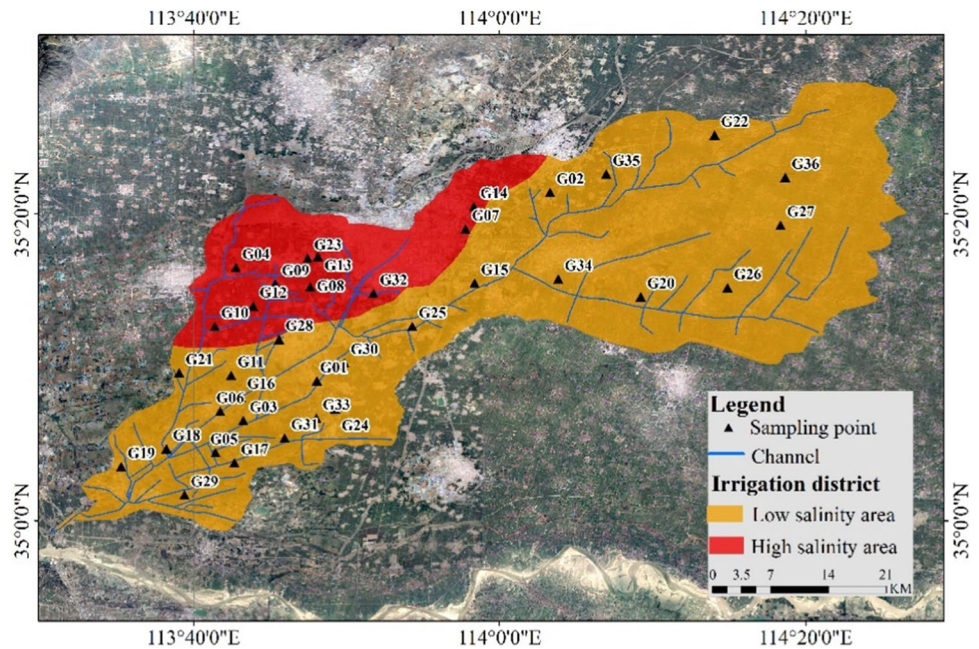


Fig. 4 Dendrogram of the Q-mode hierarchical cluster analysis

Fig. 5 The spatial distribution maps of high and low salinity area



line equation (GMWL):  $\delta D = 8.13\delta^{18}O + 10.8$ . The Yellow River water is vital in recharging groundwater in the irrigation area. The Yellow River water  $\delta D$  and  $\delta^{18}O$  values were  $-9.17\text{‰}$  and  $-65.79\text{‰}$ , respectively. The average values of  $\delta D$  and  $\delta^{18}O$  in groundwater were  $-62.7\text{‰}$

and  $-8.9\text{‰}$ , and the range was  $-73.1\text{‰} \sim -56.4\text{‰}$  and  $-10.66\text{‰} \sim -7.47\text{‰}$ , respectively. Most groundwater samples were below the LMWL (Fig. 7), similar to the Yellow River water's hydrogen and oxygen isotopic composition. This indicated that the water recharge from the Yellow River



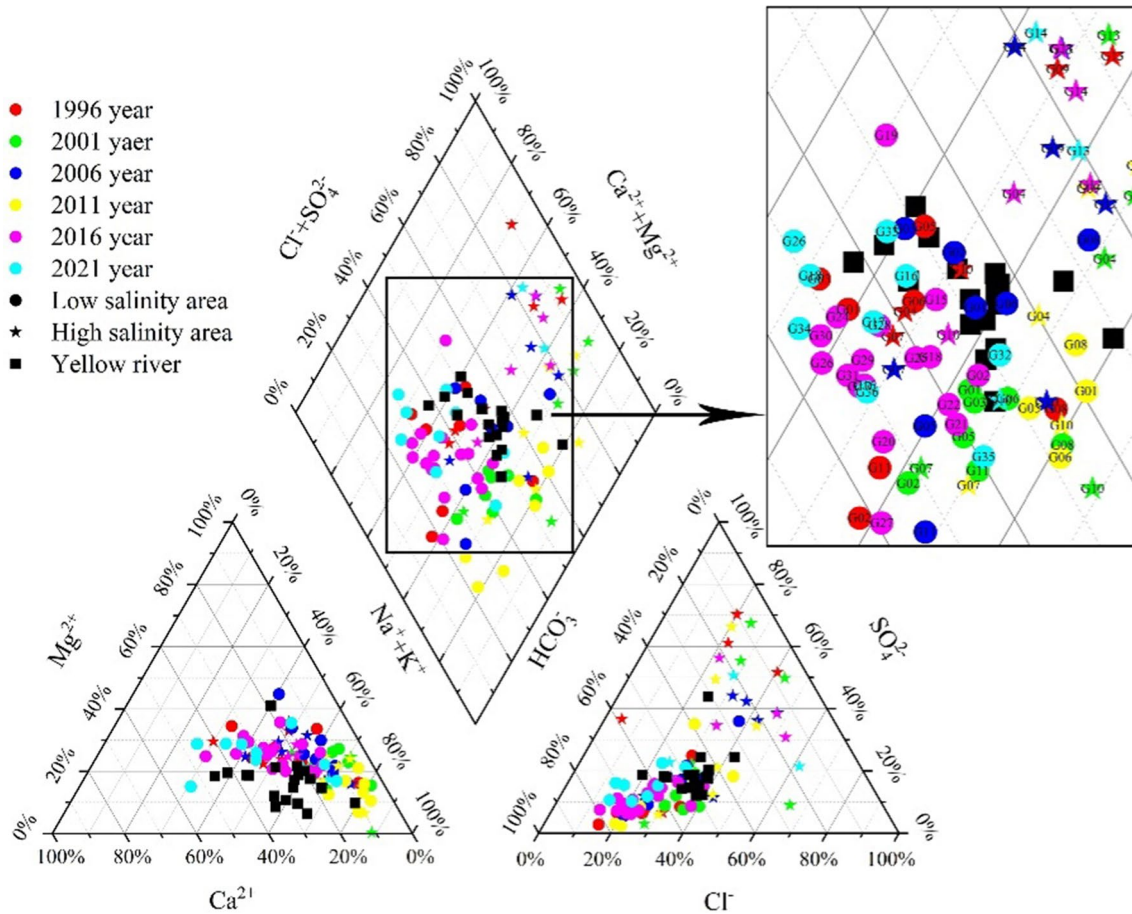


Fig. 6 The groundwater sample piper map of the study area

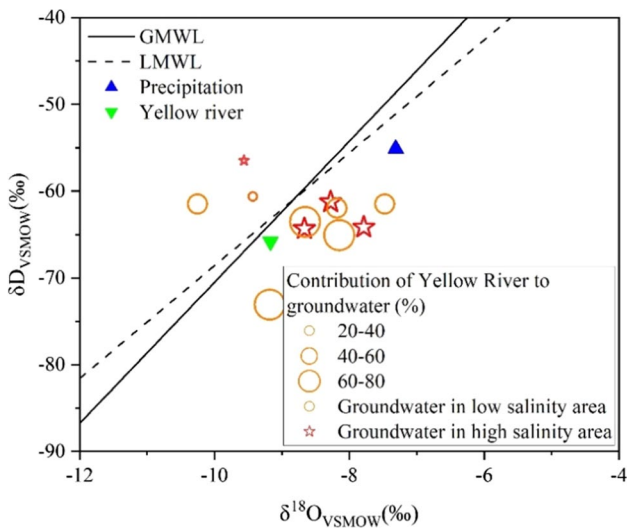


Fig. 7 Hydrogen and oxygen isotopic compositions of various water bodies and the proportion of Yellow River water recharge in groundwater

and the atmospheric precipitation are the primary sources of groundwater recharge.

The atmospheric precipitation and the Yellow River water were selected as the two endmembers of groundwater sources. The atmospheric precipitation endmember  $\delta D$  and  $\delta^{18}O$  composition values were  $-55.11\text{‰}$  and  $-7.31\text{‰}$ , and the Yellow River water endmember values were  $-62.7\text{‰}$  and  $-8.9\text{‰}$ , respectively. According to the MixSIAR Bayesian mixed model results, the groundwater in the high and low salinity areas was affected by the Yellow River water recharge. The Yellow River water recharge accounted for 50–80% in most sampling points, while the atmospheric precipitation was also a major source of groundwater recharge in the low salinity area.

### Hydrogeochemical processes

Understanding the formation mechanism of groundwater hydrochemistry is essential to discussing the relationship between groundwater and aquifer lithology in the study area (Sun et al. 2019; Wu et al. 2018; Yuan et al. 2022; Zhang et al. 2019a, b, c). In groundwater flow, a series of

reactions with the surrounding environment will result in changes in the hydrochemical composition. Yellow River water and groundwater in the low salinity area are mainly distributed in the rock weathering range (Fig. 8), indicating that rock weathering is the main factor controlling groundwater hydrochemistry. The groundwater samples in the high salinity area are close to evaporation, indicating that this process has a specific influence on salt accumulation (Chen et al. 2020; Qian et al. 2020).

Endmember diagrams were constructed to further analyze the rock types involved in the rock weathering processes driving groundwater hydrochemistry. They are composed of the  $Ca^{2+}/Na^+$  ratio against the weighted ratio of  $Mg^{2+}/Na^+$  and  $HCO_3^-/Na^+$ . Weathered sources generally include

carbonate, silicate, and evaporite (Peng et al. 2021; Zhang et al. 2022). Most of the groundwater samples in the study area were located in the weathered endmembers of silicate (Fig. 9a), indicating that silicate weathering mainly affected groundwater's chemical composition. As shown in Fig. 9b, the groundwater samples in the high salinity area were clustered to the evaporite, indicating that silicate and evaporite weathering was affecting the groundwater in the high salinity area (Wang et al. 2021a, b).

The  $Ca^{2+}$  and  $Mg^{2+}$  in natural water mainly come from carbonate weathering and the dissolution of gypsum (Fang et al. 2021; Giri et al. 2022; Zhang et al. 2019a, b, c). When the  $(Ca^{2+}/Mg^{2+}) / HCO_3^-$  ratio is 1, it indicates that  $Ca^{2+}$  and  $Mg^{2+}$  in groundwater are derived from carbonate. Most

**Fig. 8** Gibbs plot for groundwater samples in the study area and Yellow River

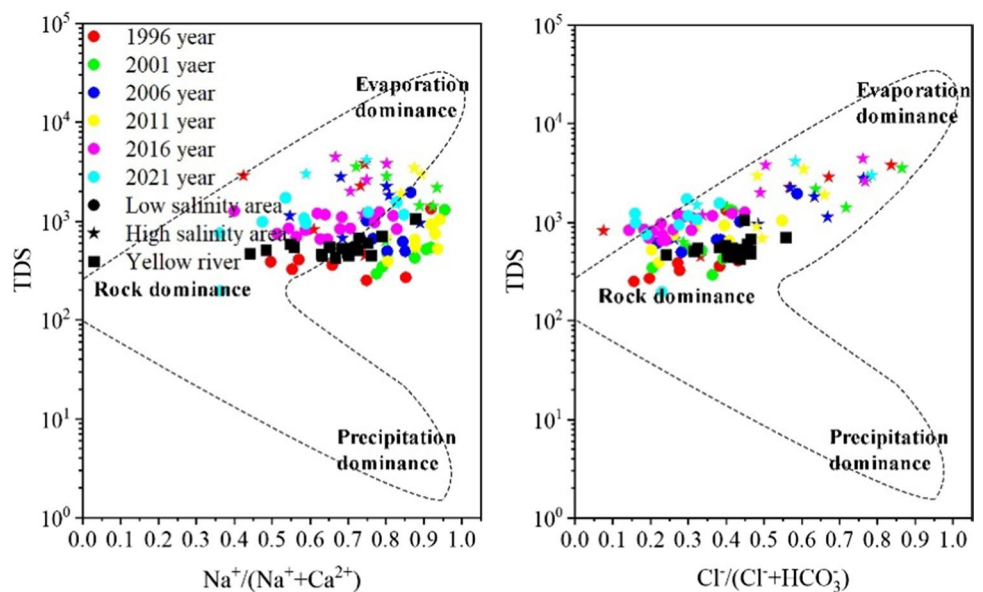
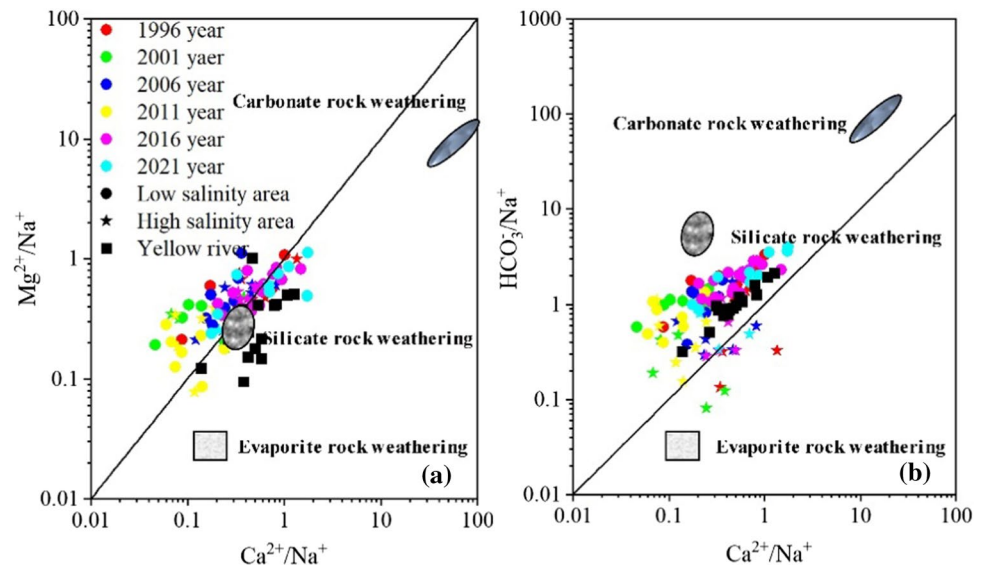


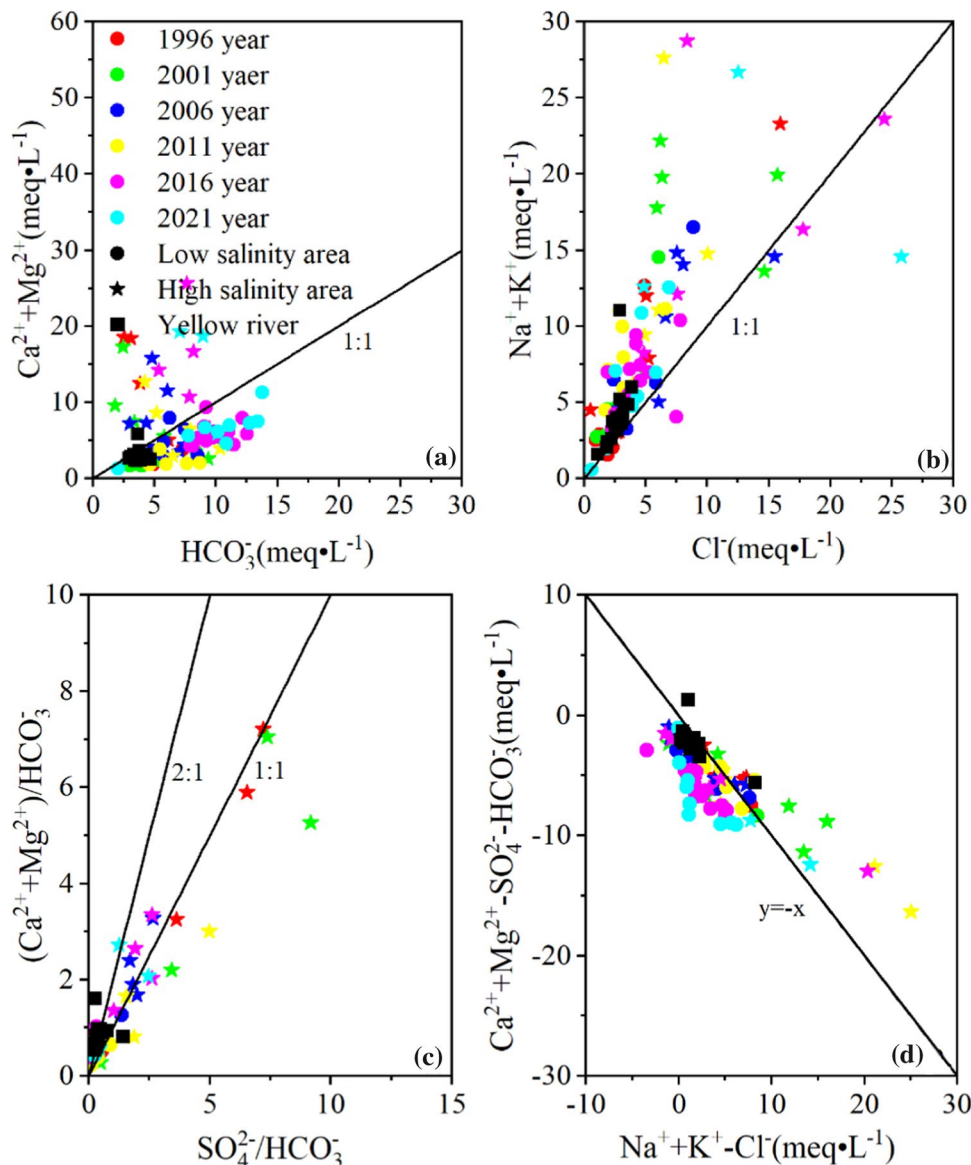
**Fig. 9** The ratio of  $Mg^{2+}/Na^+$  to  $Ca^{2+}/Na^+$ ,  $HCO_3^-/Na^+$  to  $Ca^{2+}/Na^+$  in groundwater in the study area and Yellow River



groundwater samples exhibited  $(Ca^{2+}/Mg^{2+})/HCO_3^- = 1$  (Fig. 10a), indicating that they were mainly affected by carbonate weathering. The groundwater samples in the high salinity area deviated higher than the 1 ratio, indicating that  $Ca^{2+}$  and  $Mg^{2+}$  in the high salinity area were not only from carbonate weathering, but also from evaporite, such as gypsum. Water–rock interactions play an essential role in groundwater hydrochemistry. The  $Na^+/Cl^-$  ratio is close to 1 if  $Na^+$  originates mainly from halite. When  $Na^+/Cl^- > 1$ , it means that either silicate weathering or cation exchange occurs (Lin et al. 2021; Zhao et al. 2007). Most of the groundwater samples in the study area had  $Na^+/Cl^-$  ratio value above 1 (Fig. 10b), indicating that the groundwater was mainly affected by silicate weathering. The  $(Ca^{2+}/Mg^{2+})/HCO_3^-$  to  $(SO_4^{2-}/HCO_3^-)$  ratios can be used to further analyze the carbonic acid and sulfuric acid participation in the

weathering of carbonate in groundwater. When the ratio is 1, carbonic acid is responsible for the weathering of carbonate, and when the ratio is 2, sulfuric acid is responsible for the weathering of carbonate minerals (Wang et al. 2020). As shown in Fig. 10c, the groundwater sample had ratio values between 1 and 2, indicating that both carbonic acid and sulfuric acid participate in weathering groundwater carbonate. The groundwater will exchange material with the surrounding rocks during its flow. The cations in the groundwater will be adsorbed on the rock surface due to its negative charge, releasing the original cations into the groundwater. The alternating adsorption of cations is very important to groundwater chemical evolution (Chen et al. 2021; Gao et al. 2022; Liu et al. 2022a, b). The ratio of  $(Ca^{2+} + Mg^{2+} - SO_4^{2-} - HCO_3^-)/(Na^+ + K^+ + Cl^-)$  reflects the alternating adsorption of cations. If cation exchange

**Fig. 10** Ionic relationships in groundwater in the study area and Yellow River



occurs, the above ratio is negative. Most of the groundwater sample points were distributed along a straight line with a slope of  $-1$  (Fig. 10d), indicating a profound cation exchange reaction in the groundwater.

Therefore, from the above observations, it can be concluded that the groundwater ionic components in the low salinity area were mainly derived from silicate and carbonate weathering. On the other hand, the groundwater ionic components in the high salinity area were mainly affected by silicate and evaporate weathering. The alternating adsorption of cations has an effect on the ionic composition of groundwater in the high and low salinity areas.

### Effects of atmospheric precipitation on groundwater hydrochemistry

In the low salinity area, precipitation recharge significantly affected the variation in groundwater hydrochemical composition (Fig. 11a). The  $\text{Na}^+ + \text{K}^+$ ,  $\text{Cl}^-$ ,  $\text{HCO}_3^-$  concentration and TDS in the wet season were lower than in the dry season. The mean  $\text{Na}^+ + \text{K}^+$ ,  $\text{Cl}^-$ ,  $\text{HCO}_3^-$  and TDS concentrations of the G11 groundwater sampling point in the wet season were

101.96 mg/L, 59.15 mg/L, 314.51 mg/L, and 423.20 mg/L, respectively. On the other hand, these concentrations in the dry season were 118.24 mg/L, 66.97 mg/L, 409.57 mg/L, and 506.71 mg/L, respectively. Thus, the ion concentration during the wet season was significantly lower compared to the dry season. Notably, the average annual precipitation from 1996 to 2003 was 616.81 mm, and the average precipitation from 2004 to 2013 was lower at 511.97 mm. In a similar trend, the average concentrations of other ions except for  $\text{Ca}^{2+}$  in the G06 groundwater sampling point were lower from 1996 to 2003, than from 2004 to 2013. From 1996 to 2003, the mean  $\text{Na}^+ + \text{K}^+$ ,  $\text{Cl}^-$ ,  $\text{HCO}_3^-$  and TDS concentrations were 77.97 mg/L, 70.74 mg/L, 325.28 mg/L, 380.24 mg/L, respectively, compared with 135.80 mg/L, 70.74 mg/L, 391.45 mg/L, and 532.72 mg/L from 2004 to 2013, respectively. The groundwater ion concentration decreased significantly during the years with higher precipitation. Therefore, the decrease in groundwater ion concentration through recharge by precipitation in the low salinity area is the main contributor to its chemical composition.

In the high salinity area, the variability trends between the wet and dry periods significantly differed from the low

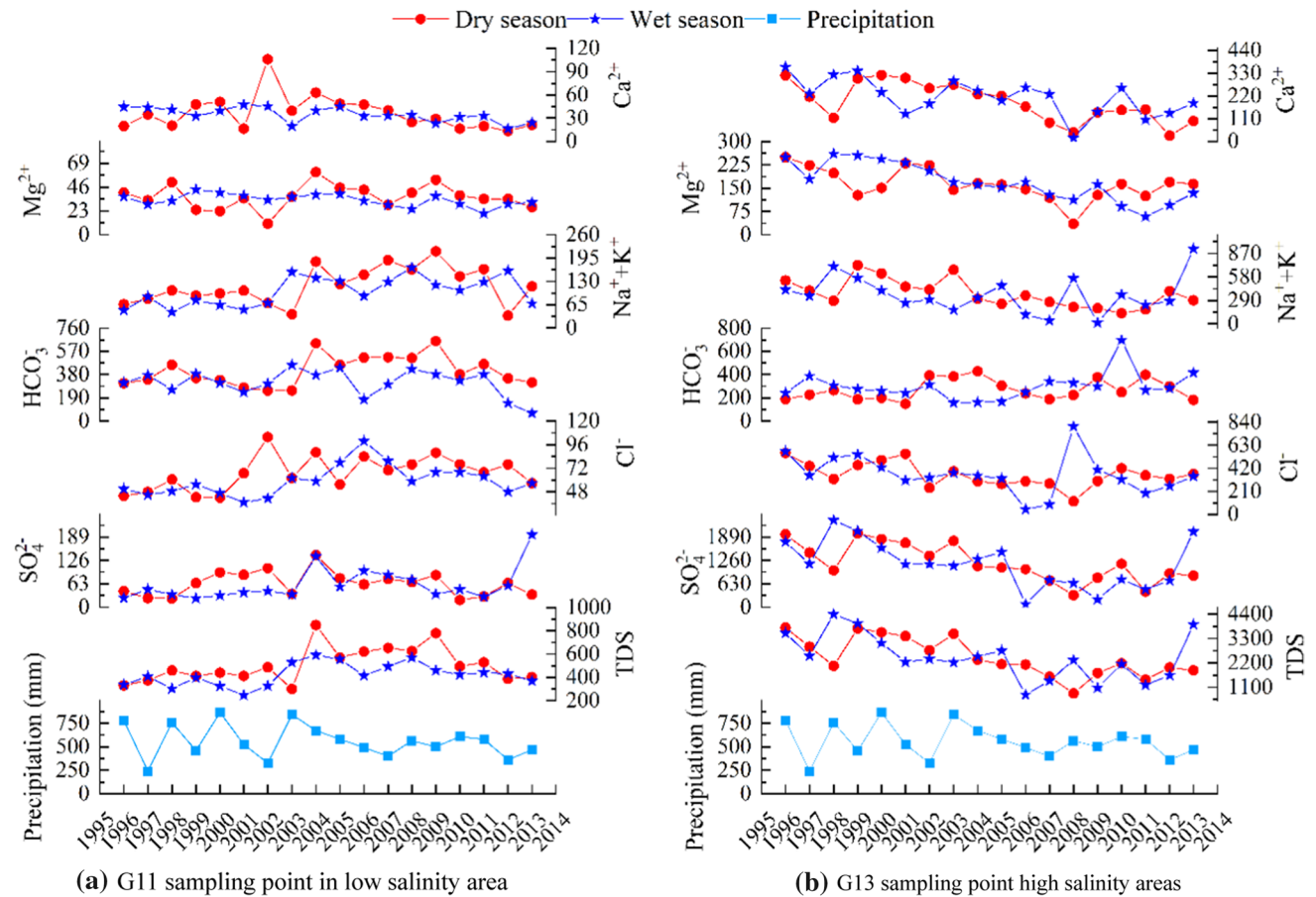


Fig. 11 Comparison of ion concentrations in groundwater during wet and dry seasons. All sample concentrations are in mg/L

salinity area (Fig. 11b). The mean  $\text{Na}^+ + \text{K}^+$  and  $\text{SO}_4^{2-}$  and TDS concentrations in the G13 groundwater sampling point during the wet season were 361.45 mg/L, 1153.39 mg/L, and 2450.19 mg/L, respectively. The values measured during the dry season were 372.17 mg/L, 1194.04 mg/L, and 2446.25 mg/L, respectively, with the average ion concentration during the wet season being similar compared to the dry season. It shows that precipitation was not the major driver for the change in groundwater hydrochemical composition. The variation of soil average ion concentration during the wet and dry seasons in the high salinity area is presented in Table 2. The high salinity area had a significantly higher average soil ion concentration than the low salinity area (Table 3). Furthermore, the average soil ion concentration in the dry season was higher than that in the wet season in the high salinity area. This indicates that in the high salinity area, soil soluble salts are leached into the aquifer with precipitation, decreasing the content of soluble salts in the soil significantly, while the concentration of solute components in groundwater increases. Therefore, the soil soluble salts leaching with precipitation into the aquifer is the main driver of the hydrochemical composition of groundwater in the high salinity area.

In conclusion, the groundwater recharge by precipitation in the low salinity areas and the ion concentration decrease are the main effects on groundwater hydrochemical composition. The soil soluble salt content was high in the high salinity area, and the soluble soil salts leaching into the aquifer with the precipitation during the wet period significantly affected the hydrochemical composition.

### Effects of yellow river irrigation on groundwater hydrochemistry

In the low salinity areas, the groundwater sampling points in proximity to the canal are affected by the direct recharge of the Yellow River. As a result, the hydrochemical composition of groundwater is comparable to that of the Yellow River. Groundwater sampling points farther away from the canal were less affected by the Yellow River. The analysis of multiple groundwater sampling points in the low salinity area far and near the canal was in accord with the above trends. The G06 and the G11 groundwater sampling points were selected as the representative points in proximity and farther away from the canal. From 1989 to 1990, the ion concentration of the G06 groundwater sampling point was relatively similar to that of the G11 groundwater sampling point (Table 4). In the G06 groundwater sampling point, the mean  $\text{Mg}^{2+}$ ,  $\text{SO}_4^{2-}$ , and  $\text{HCO}_3^-$  concentrations were 49.23 mg/L, 42.80 mg/L, and 497.23 mg/L. Similarly, in the G11 groundwater sampling point, the mean  $\text{Mg}^{2+}$ ,  $\text{SO}_4^{2-}$ , and  $\text{HCO}_3^-$  ion concentrations were 51.38 mg/L, 74.08 mg/L, and 496.80 mg/L, respectively. From 1996 to 2013, the groundwater ion concentration of the G06 groundwater sampling point gradually reached the concentration levels of the Yellow River. On the other hand, the ion concentration of the G11 groundwater sampling point differed significantly (Fig. 12a, b). The mean  $\text{Mg}^{2+}$ ,  $\text{SO}_4^{2-}$ , and  $\text{HCO}_3^-$  concentrations in the G06 groundwater sampling point were 27.38 mg/L, 127.24 mg/L, and 222.13 mg/L, respectively; 35.10 mg/L, 61.67 mg/L, 362.04 mg/L in the G11 sampling point, and 27.81 mg/L, 128.07 mg/L, and 221.33 mg/L in the Yellow River, respectively. Secondly, from 1989 to 1990, the hydrochemical types of the G06 groundwater were similar

**Table 2** Variation of soil ion concentration in wet and dry seasons in high salinity area. All sample concentrations are in mg/L

Parameter	$\text{HCO}_3^-$	$\text{Cl}^-$	$\text{SO}_4^{2-}$	$\text{Ca}^{2+}$	$\text{Mg}^{2+}$	$\text{Na}^+ + \text{K}^+$	EC
Average concentration of soil ions in dry season	46.46	16.30	122.21	23.07	8.54	42.26	940.63
Soil average concentration in wet season	61.83	13.22	92	26.91	9.54	29.07	825.50
Difference value	- 15.37	3.09	30.22	- 3.85	- 1.00	13.19	115.13

**Table 3** Variation of soil ion concentration in wet and dry seasons in low salinity area. All sample concentrations are in mg/L

Parameter	$\text{HCO}_3^-$	$\text{Cl}^-$	$\text{SO}_4^{2-}$	$\text{Ca}^{2+}$	$\text{Mg}^{2+}$	$\text{Na}^+ + \text{K}^+$	EC
Average concentration of soil ions in dry season	52.04	5.36	12.51	14.00	3.43	6.31	317.43
Soil average concentration in wet season	51.00	5.67	13.05	21.31	3.20	4.90	315.13
Difference value	1.04	- 0.30	- 0.54	- 7.31	0.22	1.42	2.30

**Table 4** Comparison of ion concentration in Yellow River water and groundwater sampling points in low salinity areas. All sample concentrations are in mg/L

Sort	Years	TDS	Ca <sup>2+</sup>	Mg <sup>2+</sup>	Na <sup>+</sup> + K <sup>+</sup>	Cl <sup>-</sup>	SO <sub>4</sub> <sup>2-</sup>	HCO <sub>3</sub> <sup>-</sup>
Yellow River	2001–2021	521.85	74.02	27.81	80.61	87.94	128.07	221.33
G06	1989–1990	543.76	55.00	49.23	90.18	59.20	42.80	497.23
	1996–2013	505.82	50.18	27.01	105.69	99.02	127.25	222.14
G11	1989–1990	594.30	57.23	51.38	102.03	74.08	61.10	496.80
	1996–2013	464.95	35.61	35.10	110.10	63.06	61.67	362.04

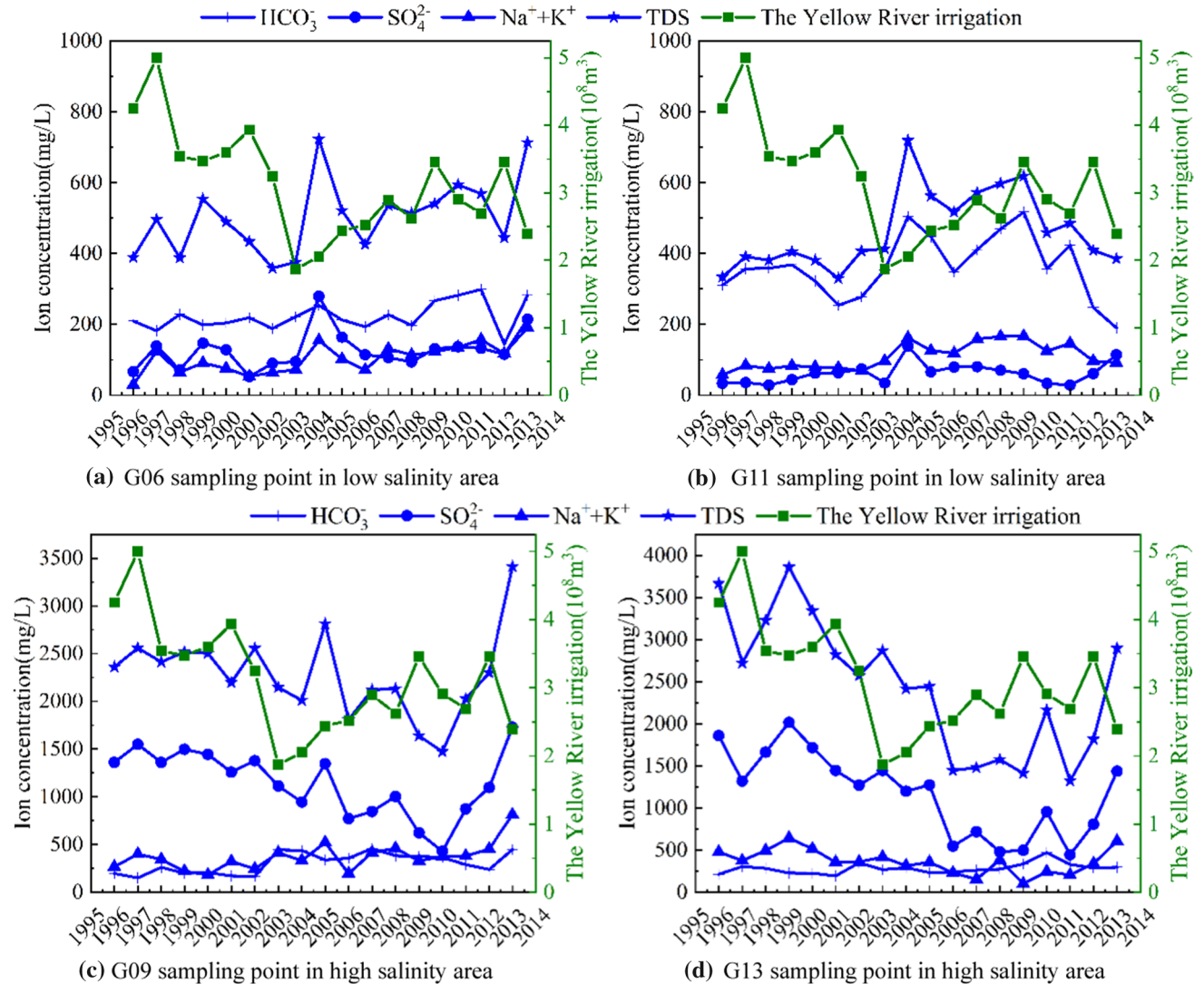


**Fig. 12** The relationship between the concentration of groundwater ions and the irrigation amount of the Yellow River in the high and low salinity area. All sample concentrations are in mg/L

to the G11 sampling point, which were HCO<sub>3</sub>-Na·Mg·Ca and HCO<sub>3</sub>-Mg·Na·Ca. From 1996 to 2013, the G06 groundwater sampling point hydrochemical types were mainly HCO<sub>3</sub>-Cl-Na·Ca and HCO<sub>3</sub>·SO<sub>4</sub>-Na·Mg. The hydrochemical types of the Yellow River sampling points were HCO<sub>3</sub>-Cl-Na·Ca, and HCO<sub>3</sub>·SO<sub>4</sub>-Ca·Na, while in the G06 groundwater sampling point, they were similar to those of

the Yellow River. The G11 groundwater sampling point hydrochemical types were mainly HCO<sub>3</sub>-Na·Mg·Ca, and HCO<sub>3</sub>-Cl-Na·Mg, which differed from the hydrochemical types of the Yellow River and the G06 groundwater sampling points. Therefore, the Yellow River directly recharges the groundwater in the low salinity area close to the canal,

resulting in ion concentrations similar to that of the Yellow River.

The water is diverted from the Yellow River in the high salinity area, effectively desalinating the groundwater close to the canal. When the water volume diverted from the Yellow River is large, the groundwater sampling points closer to the canal are more affected by this desalination process. On the other hand, when a lower volume of water is diverted, the desalination effect of the Yellow River water on the high salinity area is significantly reduced. The ion concentration of the G09 groundwater sampling point from 1996 to 2013, closer to the canal, was slightly lower than that of G13 (Fig. 12c, d). Especially in 1996–2003, when the volume of water diverted from the Yellow River was large, the ion concentration of the G09 groundwater sampling point was significantly lower than that of the G13 (Table 5). The  $\text{Na}^+ + \text{K}^+$ ,  $\text{Cl}^-$  and TDS concentration in the G09 groundwater sampling point were 0.34%, 0.56%, and 0.23% lower than the G13 groundwater sampling point. When the volume of water diverted from the Yellow River is small, the recharge volume to the groundwater is similarly small. To conclude, the Yellow River water is not the main factor affecting the groundwater hydrochemistry in the high salinity area. Therefore, when the Yellow River water recharge is large in the high salinity area, it recharges the groundwater in proximity to the canal to reduce its ion concentration, significantly reducing the groundwater hydrochemical composition. The Yellow River recharge is not the main factor affecting groundwater ion concentration when the recharge volume is small.

The Yellow River significantly impacts groundwater near the irrigation canal. In the low salinity area, the Yellow River recharge affects the ion concentration in the groundwater close to the canal, making it similar to the Yellow River. In the high salinity area, as the Yellow River ion concentration is lower than the groundwater, its recharge reduces the groundwater ion concentration closer to the canal.

### Effects of groundwater exploitation on groundwater hydrochemistry

In the low salinity area, before the landing funnel formation at the G24 sampling point in 2003, the ion concentration

at the G01 sampling point was low (Fig. 13a). The mean concentration of  $\text{Na}^+ + \text{K}^+$ ,  $\text{SO}_4^{2-}$  ions and TDS were 65.80 mg/L, 52.78 mg/L, and 362.00 mg/L, respectively, at the G01 groundwater sampling sites from 1996 to 2003. These concentrations increased gradually after the formation of a depression at the G24 groundwater sampling site in 2003. The mean concentration of  $\text{Na}^+ + \text{K}^+$ ,  $\text{SO}_4^{2-}$  ions and TDS increased 134.63 mg/L, 166.57 mg/L, and 622.04 mg/L, respectively, at the G01 groundwater sampling sites from 2004 to 2013. The mean concentration of  $\text{Na}^+ + \text{K}^+$ ,  $\text{SO}_4^{2-}$  ions and TDS during 2004–2013 increased by 104%, 215%, and 71%, respectively, compared with those during 1996–2003. The increase of exploitation near the G24 groundwater sampling point leads to the formation of a depression cone, causing the direction of groundwater flow to change. The groundwater from the high salinity area flows to the G24 sampling point, increasing groundwater ion concentration in the low salinity area.

In the high salinity area, the ion concentration in the G13 groundwater sampling point before 2003 was relatively high (Fig. 13b). The mean concentration of  $\text{Na}^+ + \text{K}^+$ ,  $\text{SO}_4^{2-}$  ions and TDS were 456.37 mg/L, 1593.40 mg/L, and 3134.84 mg/L, respectively, in the G13 groundwater sampling sites from 1996 to 2003.  $\text{Na}^+ + \text{K}^+$ ,  $\text{SO}_4^{2-}$  and TDS concentration at the G13 groundwater sampling sites decreased after 2003. The mean ion and TDS concentrations of the G13 groundwater sampling sites from 2004 to 2013 were 295.16 mg/L, 837.96 mg/L, and 1898.93 mg/L, respectively. Mean  $\text{Na}^+ + \text{K}^+$ ,  $\text{SO}_4^{2-}$  and TDS concentration were decreased by 35%, 47%, and 39%, respectively. After 2003, the groundwater in the high salinity area flowed to a regional drawdown funnel, the flow rate increased, and the groundwater ion concentration in the high salinity area decreased.

In conclusion, the groundwater production increase causes a change in the flow direction and has a significant impact on local groundwater chemistry. As the groundwater flows through the high salinity area, it increases the groundwater ions concentration in the low salinity area. On the other hand, the groundwater of the high salinity area flows to the funnel area, and the flow rate increases, which results in a groundwater ion concentration decrease in the high salinity area.

**Table 5** Comparison of ion concentrations in groundwater sampling points in high salinity areas. All sample concentrations are in mg/L

Sort	Years	TDS	$\text{Ca}^{2+}$	$\text{Mg}^{2+}$	$\text{Na}^+ + \text{K}^+$	$\text{Cl}^-$	$\text{SO}_4^{2-}$	$\text{HCO}_3^-$
G09	1996–2013	2277.50	142.55	169.37	371.69	251.19	1146.97	305.58
	1996–2003	2406.53	182.52	184.95	300.45	191.34	1371.25	225.27
	2004–2013	2174.27	110.58	156.91	428.68	299.07	967.55	369.83
G13	1996–2013	2448.22	202.97	166.19	366.81	362.74	1173.71	284.59
	1996–2003	3134.84	263.22	208.88	456.37	430.56	1593.40	260.26
	2004–2013	1898.93	154.77	132.03	295.16	308.49	837.96	304.05

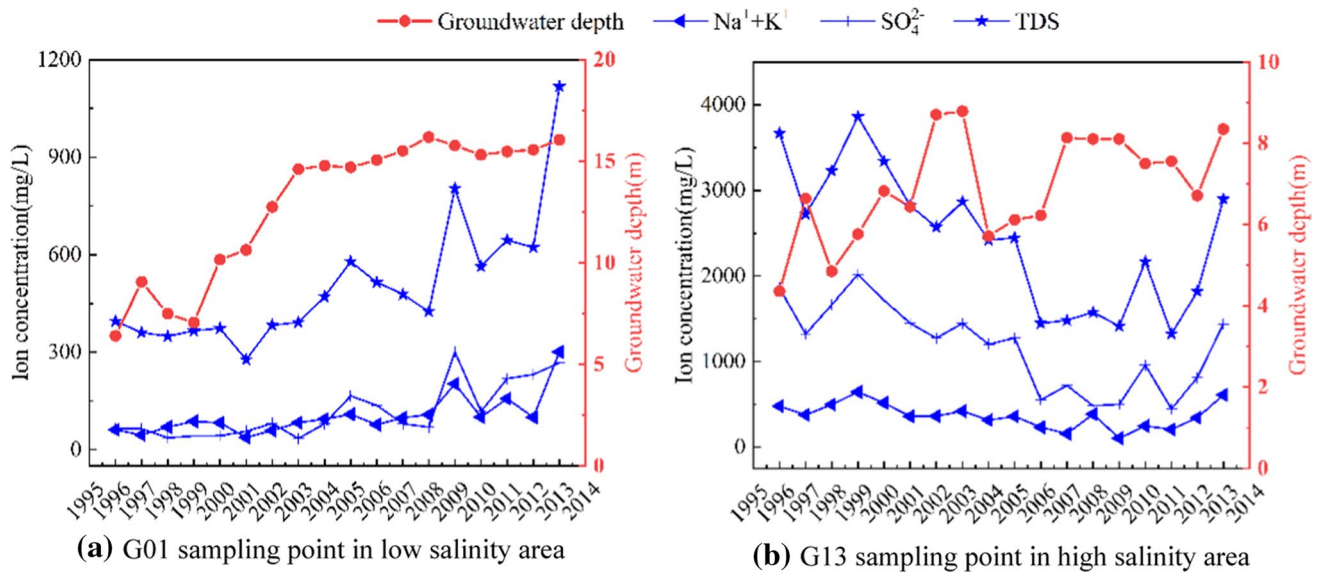


**Fig. 13** Interannual variation of groundwater ion concentration and groundwater depth in high and low salinity area

## Conclusion

The groundwater ion concentration in the study area had prominent spatial zoning characteristics. Specifically, it was divided into two areas: the high salinity northwest area, while the other areas had low salinity. The groundwater in the high salinity area had a higher concentration of  $\text{Na}^+$ ,  $\text{Cl}^-$ , and  $\text{SO}_4^{2-}$ , the water type was  $\text{SO}_4\text{-Cl-Na-Mg}$ , while in the low salinity area, the water type was  $\text{HCO}_3\text{-Cl-Na-Mg}$  and  $\text{HCO}_3\text{-Na-Ca}$ .

The study area mainly originated from rock weathering processes. Specifically, they mainly originated from silicate and carbonate weathering in the low salinity area. In the high salinity area, silicate and evaporite weathering were the main sources of groundwater ions.

The variation of groundwater ion concentration in the low salinity area was mainly affected by the Yellow River water, atmospheric precipitation, and partially by the amount of exploitation. The soil soluble salt content was low in the low salinity area. The main effect of precipitation on groundwater chemical composition is to reduce the ion concentration by recharge. The groundwater ion concentration near the canal was similar to that of the Yellow River. The G24 groundwater sampling point in 2003 formed a landing hopper of groundwater, and the groundwater flow direction changed, resulting in an increase in groundwater ion concentration in the area passing through the groundwater flow from the high-salinity area to the low-salinity area.

The groundwater ion concentration changes in the high salinity areas were due to more complex processes, with the leaching of soluble soil salts being the dominant factor

causing the change in groundwater chemistry. In addition, precipitation, Yellow River water diversion, and exploitation affected the groundwater ion concentration. The soil soluble salt concentration in the high salinity area was high, and they were leached into the aquifer by precipitation during the wet period. This process increased the concentration of solute components in the groundwater. The Yellow River recharge decreased the groundwater ion concentration near the canal. After 2003, the groundwater in the high salinity area flowed to the funnel area, and its flow rate increased, resulting in a decreased groundwater ion concentration in the high salinity area.

**Acknowledgements** The author is sincerely thankful to all the editors and reviewers for their suggestions for further refining the quality of this study.

**Funding** Innovative Research Group Project of the National Natural Science Foundation of China, 42072287, Zhongpei Liu, North China University of Water Resources and Electric Power, YK-2021-47, Shaoyi Feng

## Declarations

**Conflict of interest** All authors declare that they have no conflict of interest.

**Ethical approval** This article does not contain any studies with human participants or animals performed by any of the authors.

**Open Access** This article is licensed under a Creative Commons Attribution 4.0 International License, which permits use, sharing, adaptation, distribution and reproduction in any medium or format, as long as you give appropriate credit to the original author(s) and the source, provide a link to the Creative Commons licence, and indicate if changes were made. The images or other third party material in this article are



included in the article's Creative Commons licence, unless indicated otherwise in a credit line to the material. If material is not included in the article's Creative Commons licence and your intended use is not permitted by statutory regulation or exceeds the permitted use, you will need to obtain permission directly from the copyright holder. To view a copy of this licence, visit <http://creativecommons.org/licenses/by/4.0/>.

## References

- Abdalla FA, Scheytt T (2012) Hydrochemistry of surface water and groundwater from a fractured carbonate aquifer in the Helwan area. *Egypt J Earth Syst Sci* 121(1):109–124. <https://doi.org/10.1007/s12040-012-0140-7>
- Ahmad S, Singh N, Mazhar SN (2020) Hydrochemical characteristics of the groundwater in Trans-Yamuna Alluvial aquifer, Palwal district, Haryana India. *Appl Water Sci* 10(2):75. <https://doi.org/10.1007/s13201-020-1150-2>
- Aksever F, Davraz A, Bal Y (2016) Assessment of water quality for drinking and irrigation purposes: a case study of Baskoy springs (Aglasun/Burdur/Turkey). *Arab J Geosci*. <https://doi.org/10.1007/s12517-016-2778-y>
- Aragaw TT, Gnanachandrasamy G (2021) Evaluation of groundwater quality for drinking and irrigation purposes using GIS-based water quality index in urban area of Abaya-Chemo sub-basin of Great Rift Valley Ethiopia. *Appl Water Sci*. <https://doi.org/10.1007/s13201-021-01482-6>
- Asmael NM, Huneau F, Garel E, Celle-Jeanton H, Le Coustumer P, Dupuy A (2014) Hydrochemistry to delineate groundwater flow conditions in the Mogher Al Mer area (Damascus Basin, South-western Syria). *Environ Earth Sci* 72(8):3205–3225. <https://doi.org/10.1007/s12665-014-3226-5>
- Azevedo CJEG (2021) Flow patterns and aquifer recharge controls under Amazon rainforest influence: the case of the Alter do Chao aquifer system. *J S Am Earth Sci*. <https://doi.org/10.1016/j.jsames.2021.103596>
- Ben Ammar S, Taupin JD, Zouari K, Khouatmia M (2016) Identifying recharge and salinization sources of groundwater in the Oussja Ghar el Melah plain (northeast Tunisia) using geochemical tools and environmental isotopes. *Environ Earth Sci*. <https://doi.org/10.1007/s12665-016-5431-x>
- Bodrud-Doza M, Islam ARMT, Ahmed F, Das S, Saha N, Rahman MS (2016) Characterization of groundwater quality using water evaluation indices, multivariate statistics and geostatistics in central Bangladesh. *Water Sci* 30(1):19–40. <https://doi.org/10.1016/j.wsj.2016.05.001>
- Chang XM, Wang SL, Chen GR, Fu XJ, Xu NN, Yang XP (2018) Spatiotemporal changes and influencing factors of soil salinity in Hetao irrigation district. *J Drain Irrig Mach Eng* 36(10):1000–1005
- Chen J, Qian H, Gao YY, Wang HK, Zhang MS (2020) Insights into hydrological and hydrochemical processes in response to water replenishment for lakes in arid regions. *J Hydrol*. <https://doi.org/10.1016/j.jhydrol.2019.124386>
- Chen J, Gao YY, Qian H, Ren WH, Qu WG (2021) Hydrogeochemical evidence for fluoride behavior in groundwater and the associated risk to human health for a large irrigation plain in the Yellow River Basin. *Sci Total Environ*. <https://doi.org/10.1016/j.scitotenv.2021.149428>
- Cheng CH, Deng YX, Zhuo XK, Dai D, Yu T (2021) Changes in water chemistry and driving factors in the middle and lower reaches of the Beijing-Hangzhou grand canal. *Environ Sci* 42(05):2251–2259. <https://doi.org/10.13227/j.hjcx.202009018>
- Cui JQ, Li XY, Shi HB, Sun YN, An HJ, Xing JP (2020) Chemical evolution and formation mechanism of groundwater in Hetao irrigation area. *Environ Sci* 41(09):4011–4020. <https://doi.org/10.13227/j.hjcx.202003150>
- Cui YH, Wang J, Liu YC, Hao S, Gao X (2021) Hydro-chemical characteristics and ion origin analysis of surface-groundwater in the meeting place of Shengjin lake and Yangtze river. *Environ Sci* 42(07):3223–3231. <https://doi.org/10.13227/j.hjcx.202012016>
- El Alfy M, Abdalla F, Moubark K, Alharbi T (2019) Hydrochemical equilibrium and statistical approaches as effective tools for identifying groundwater evolution and pollution sources in arid areas. *Geosci J* 23(2):299–314. <https://doi.org/10.1007/s12303-018-0039-7>
- Fan BL, Zhang D, Tao ZH, Zhao ZQ (2017) Compositions of hydrogen and oxygen isotope values of Yellow River water and the response to climate change. *China Environ Sci* 37(05):1906–1914
- Fang LJ, Gao RZ, Jia DB, Yu RH, Liu XY, Liu TX (2021) Spatial-temporal characteristics of groundwater quality and its environmental driving factors of Steppe Basin—taken Balaguer river basin of inner Mongolia for instance. *China Environ Sci* 41(05):2161–2169. <https://doi.org/10.19674/j.cnki.issn1000-6923.20210330.001>
- Feng XB, Xiao K, Li HL (2020) Tidal groundwater flow and its potential effect on the hydrochemical characteristics in a mud-sand-layered aquifer in Daya Bay China. *Environ Sci Pollut Res* 27(19):24438–24451. <https://doi.org/10.1007/s11356-020-08809-x>
- Gao YY, Chen J, Qian H, Wan HK, Ren WH, Qu WG (2022) Hydrogeochemical characteristics and processes of groundwater in an over 2260 year irrigation district: a comparison between irrigated and nonirrigated areas. *J Hydrol*. <https://doi.org/10.1016/j.jhydrol.2022.127437>
- Giri A, Bharti VK, Kalia S, Kumar K, Khansu M (2022) Hydrochemical and quality assessment of irrigation water at the trans-himalayan high-altitude regions of Leh, Ladakh, India. *Appl Water Sci*. <https://doi.org/10.1007/s13201-022-01716-1>
- Guo XJ, Wang WH, Wang JS, Wang W (2022) Hydrochemical characteristics and evolution pattern of groundwater system in Baiyangdian wetland North Chian Plain. *Acta Geol Sin* 96(02):656–672. <https://doi.org/10.19762/j.cnki.dizhixuebao.2021061>
- He ZH, Unger-Shayesteh K, Vorogushyn S, Weise SM, Duethmann D, Kalashnikova O et al (2020) Comparing Bayesian and traditional end-member mixing approaches for hydrograph separation in a glacierized basin. *Hydrol Earth Syst Sci* 24(6):3289–3309. <https://doi.org/10.5194/hess-24-3289-2020>
- Heleika MA, Toney S, Ismail E (2021) Mapping of groundwater opportunities for multi-purposes use in Beni-Suef province Egypt. *Arab J Geosci* 14(9):784. <https://doi.org/10.1007/s12517-021-07123-1>
- Huang JZ, Xian Y, Li W, Zhang DZ, Zhuang XM (2021) Hydrogeochemical evolution of groundwater flow system in the typical coastal plain: a case study of Hangjiahu plain. *Earth Sci* 46(07):2565–2582
- Keesari T, Pant D, Roy A, Sinha UK, Jaryal A, Singh M et al (2021) Fluoride geochemistry and exposure risk through groundwater sources in Northeastern parts of Rajasthan, India. *Arch Environ Contam Toxicol* 80(1):294–307. <https://doi.org/10.1007/s00244-020-00794-z>
- Khanoranga KS (2019) An assessment of groundwater quality for irrigation and drinking purposes around brick kilns in three districts of Balochistan province, Pakistan, through water quality index and multivariate statistical approaches. *J Geochem Explor* 197:14–26. <https://doi.org/10.1016/j.gexplo.2018.11.007>
- Lecomte KL, Bicalho CC, Silva EV (2016) Geochemical characterization in karst basin tributaries of the San Franciscan depression: the Corrente river, western Bahia, NE-Brazil. *J S Am Earth Sci* 69:119–130. <https://doi.org/10.1016/j.jsames.2016.03.011>

- Li P, Nurolla M, Liang ZJ, Huang ZD, Qi XB (2017) Effects of canal well water ratios on root layer soil desalination and groundwater hydrochemical characteristics. *Sci Agric Sin* 50(03):526–536
- Li PY (2014) Research on groundwater environment under human interferences: a case study from weining plain, Northwest China. Dissertation, Chang'an University
- Lin CY, Sun ZX, Gao B, Hua EX, Zhang HY, Yang F et al (2021) Hydrochemical characteristics and formation mechanism of groundwater in Lhasa Area China. *Earth Sci Front* 28(05):49–58. <https://doi.org/10.13745/j.esf.sf.2021.2.2>
- Liu JT, Gao ZJ, Wang M, Li YZ, Ma YY, Shi MJ et al (2018a) Study on the dynamic characteristics of groundwater in the valley plain of Lhasa city. *Environ Earth Sci* 77(18):646. <https://doi.org/10.1007/s12665-018-7833-4>
- Liu ZP, Zhao YT, Han YP, Wang CY, Wang FQ (2018b) Driving factors of the evolution of groundwater level in People's Victory Canal Irrigation District China. *Desalin Water Treat* 112:324
- Liu X, Xiang W, Si BC (2021) Hydrochemical and isotopic characteristics in the shallow groundwater of the Fenhe river basin and indicative significance. *Environ Sci* 42(04):1739–1749. <https://doi.org/10.13227/j.hjck.202008315>
- Liu F, Zou JW, Liu JR, Zhang JK, Zhen PN (2022a) Factors controlling groundwater chemical evolution with the impact of reduced exploitation. *CATENA*. <https://doi.org/10.1016/j.catena.2022.106261>
- Liu ZP, Qi MK, Han YP, Cao RX, Leng J (2022b) Prediction of groundwater depression cone based on EMD-AR model in the irrigation area of the Lower Yellow River. *J Henan Normal Univ* 50(03):29–38
- Ma HY, Zhu GF, Zhang Y, Sang LY, Wan QZ, Zhang ZY et al (2021) Ion migration process and influencing factors in inland river basin of arid area in China: a case study of Shiyang River Basin. *Environ Sci Pollut Res* 28(40):56305–56318. <https://doi.org/10.1007/s11356-021-14484-3>
- Okkonen J, Kløve B (2012) Assessment of temporal and spatial variation in chemical composition of groundwater in an unconfined esker aquifer in the cold temperate climate of Northern Finland. *Cold Reg Sci Technol* 71:118–128. <https://doi.org/10.1016/j.coldreg.2011.10.003>
- Peng HX, Hou QQ, Zeng M, Huang CS, Shi HH, Pi PC et al (2021) Hydrochemical characteristics and controlling factors of groundwater in Leizhou Peninsula. *Environ Sci* 42(11):5375–5383. <https://doi.org/10.13227/j.hjck.202104073>
- Piper AM (1944) A graphic procedure in the geochemical interpretation of water-analyses. *EOS Trans Am Geophys Union* 25(6):914–928. <https://doi.org/10.1029/TR025i006p00914>
- Qian H, Chen J, Howard KWF (2020) Assessing groundwater pollution and potential remediation processes in a multi-layer aquifer system. *Environ Pollut*. <https://doi.org/10.1016/j.envpol.2020.114669>
- Qu B, Zhang YL, Kang SC, Sillanpää M (2019) Water quality in the Tibetan Plateau: major ions and trace elements in rivers of the “Water Tower of Asia.” *Sci Total Environ* 649:571–581. <https://doi.org/10.1016/j.scitotenv.2018.08.316>
- Rahman T, Mat M, Saadat AHM, Islam MS, Al-Mansur MA, Ahmed S (2017) Groundwater characterization and selection of suitable water type for irrigation in the western region of Bangladesh. *Appl Water Sci* 7(1):233–243. <https://doi.org/10.1007/s13201-014-0239-x>
- Ran JY, Zhang JX (2018) Investigation and comparison on hydrochemistry characteristic of typical basin in urt Moron. *Environ Sci* 36(06):73–77. <https://doi.org/10.13205/j.hjgc.201806016>
- Rodriguez M, Ohlanders N, Pellicciotti F, Williams MW, McPhee J (2016) Estimating runoff from a glacierized catchment using natural tracers in the semi-arid Andes cordillera. *Hydrol Process* 30(20):3609–3626. <https://doi.org/10.1002/hyp.10973>
- Sharma SK, Yadav S, Parashar VK, Dubey P (2018) Assessment of agricultural water quality of shallow groundwater between Budhni and Chaurasakhed, North of River Narmada, District Sehore, Madhya Pradesh, India. Paper presented at the Environmental Pollution, Singapore.
- Sun CJ, Yang W, Chen RX, Hou HX, Zheng ZJ (2019) Spatiotemporal changes in hydro-chemistry of groundwater in irrigation district within the Kaidu River basin. *J Irrig Drain* 38(07):84–93. <https://doi.org/10.13522/j.cnki.ggps.20180682>
- Tirumalesh K, Shivanna K, Sriraman AK, Tyagi AK (2010) Assessment of quality and geochemical processes occurring in groundwaters near central air conditioning plant site in Trombay, Maharashtra India. *Environ Monit Assess* 163(1):171–184. <https://doi.org/10.1007/s10661-009-0825-9>
- Tran DA, Tsujimura M, Vo LP, Nguyen VT, Nguyen LD, Dang TD (2019) Stable isotope characteristics of water resources in the coastal area of the Vietnamese Mekong Delta. *Isot Environ Health Stud* 55(6):566–587. <https://doi.org/10.1080/10256016.2019.1673746>
- Tyagi SK, Datta PS, Pruthi NK (2009) Hydrochemical appraisal of groundwater and its suitability in the intensive agricultural area of Muzaffarnagar district, Uttar Pradesh India. *Environ Geol* 56(5):901–912. <https://doi.org/10.1007/s00254-008-1190-7>
- Wang YJ, Song XF, Li BH, Ma Y, Zhang YH, Yang LH et al (2018) Temporal variation in groundwater hydrochemistry driven by natural and anthropogenic processes at a reclaimed water irrigation region. *Hydrol Res* 49(5):1652–1668. <https://doi.org/10.2166/nh.2018.123>
- Wang YS, Li S, Li HX, Cheng XX, Li WP, Zhang MN (2019) Groundwater salinization characteristics and controlling factors in the Haiyuan Basin. *Hydrogeol Eng Geol* 46(04):10–17. <https://doi.org/10.16030/j.cnki.issn.1000-3665.2019.04.02>
- Wang P, Jing MG, Lu DC (2020) Hydrogeochemistry characteristics and formation mechanism of shallow groundwater in Yongcheng City Henan Province. *Earth Sci* 45(06):2232–2244
- Wang WR, Chen YN, Wang WH, Xia ZH, Li XY, Kayumba PM (2021a) Hydrochemical characteristics and evolution of groundwater in the dried-up river oasis of the Tarim Basin. *Central Asia J Arid Land* 13(10):977–994. <https://doi.org/10.1007/s40333-021-0086-1>
- Wang WX, Li WP, Cai YM, An YH, Shao XM, Wu X et al (2021b) The hydrogeochemical evolution of groundwater in the middle reaches of the Heihe River Basin. *Earth Sci Front* 28(04):184–193. <https://doi.org/10.13745/j.esf.sf.2021.5.28>
- Wu YZ, Pan CF, Lin Y, Cao FL, Wang ZJ (2018) Hydrogeochemical characteristics and controlling factors of main water filled aquifers in the typical North China coalfield. *Bull Geol Sci Technol* 37(05):191–199. <https://doi.org/10.19509/j.cnki.dzqk.2018.0526>
- Xiong GY, Chen GQ, Xu XY, Liu WQ, Fu TF, Khokiattiwong S et al (2020) A comparative study on hydrochemical evolution and quality of groundwater in coastal areas of Thailand and Bangladesh. *J Asian Earth Sci* 195:104336. <https://doi.org/10.1016/j.jseaes.2020.104336>
- Xu XL, Li YL, Gao B, Zhang YB (2022) Composition of water sources and transformation relationship between surface water and groundwater in the Fenhe River estuarine wetland of the middle-Yellow River. *J Lake Sci* 34(01):247–261
- Yang QC, Li ZJ, Xie C, Liang J, Ma HY (2020) Risk assessment of groundwater hydrochemistry for irrigation suitability in Ordos Basin China. *Nat Hazards* 101(2):309–325. <https://doi.org/10.1007/s11069-018-3451-4>
- Yuan HY, Yang SQ, Wang B (2022) Hydrochemistry characteristics of groundwater with the influence of spatial variability and water flow in Hetao irrigation district, China. *Environ Earth Sci* 1:1–17. <https://doi.org/10.1007/s11356-022-20685-1>

- Zhang JX, Qi XB, Nurolla M, Li P, Huang ZD, Hu YL (2017) Appropriate Well-canal Irrigation Proportion in Irrigation District Based on MODFLOW and GIS. *J Irrig Drain* 36(02):58–63. <https://doi.org/10.13522/j.cnki.ggps.2017.02.009>
- Zhang J, Wang WK, Wang XY, Yin LH, Zhu LF, Sun FQ et al (2019a) Seasonal variation in the precipitation recharge coefficient for the Ordos Plateau Northwest China. *Hydrogeol J* 27(2):801–813. <https://doi.org/10.1007/s10040-018-1891-2>
- Zhang XJ, Wang P, Wang TY, Yu JJ, Liu X (2019b) Relationship between chemical characteristics of shallow groundwater and water level depth in Ejian Oasis under water conveyance conditions. *South-to-North Water Transf Water Sci Technol* 17(06):86–94. <https://doi.org/10.13476/j.cnki.nsbdqk.2019.0139>
- Zhang Y, Guo CQ, Zhu YG, Yu S (2019c) Chemical characteristics of groundwater and material sources analysis in Buckwheat field Yunnan Province. *Environ Sci* 40(06):2686–2695. <https://doi.org/10.13227/j.hjkk.201810229>
- Zhang Y, Cheng R, Zou L, Liang ZJ, Lv W, Dou M et al (2022) The effects of climate change and anthropogenic activities on groundwater in irrigation district. *J Irrig Drain* 41(02):91–100. <https://doi.org/10.13522/j.cnki.ggps.2021435>
- Zhao XF, Chen JNY, Tang CY, Zeng SQ, Lu YT (2007) Hydrochemical characteristics and evolution of groundwater in a small catchment of Pearl River Delta. *Ecol Environ Sci* 06:1620–1626. <https://doi.org/10.16258/j.cnki.1674-5906.2007.06.004>

**Publisher's Note** Springer Nature remains neutral with regard to jurisdictional claims in published maps and institutional affiliations.